



PAPER

Structural damage identification with output-only strain measurements and swarm intelligence algorithms: a comparative study

To cite this article: Guangcai Zhang *et al* 2024 *Meas. Sci. Technol.* **35** 056125

View the [article online](#) for updates and enhancements.

You may also like

- [Java Algorithm for Optimization of Cooling Slope Casting Process Parameters](#)
Rahaini Mohd Said, Roselina Sallehuddin, Nor Haizan Mohd Radzi et al.
- [Experimental investigation on cladding with metal cored wire using GMAW process and parametric optimization](#)
Ashish Kaushik, Vivek Singh, Bishub Choudhury et al.
- [Deformation health diagnosis of RCC dams considering construction interfaces based on monitoring data and numerical simulation](#)
Xudong Chen, Liuyang Li, Yajian Liu et al.

The Breath Biopsy[®] Guide
Fourth edition

FREE




DOWNLOAD THE FREE E-BOOK

BREATH BIOPSY[®]

OWLSTONE MEDICAL

The advertisement features a dark blue background with a white molecular structure pattern in the top right. On the left, a tablet displays the book cover for 'The Breath Biopsy Guide Fourth edition'. A white starburst graphic with the word 'FREE' is positioned next to the book cover. Below the book cover is a blue button with the text 'DOWNLOAD THE FREE E-BOOK'. To the right of the button are two logos: 'BREATH BIOPSY' in an orange box and 'OWLSTONE MEDICAL' in a white box with a blue circular icon.

Structural damage identification with output-only strain measurements and swarm intelligence algorithms: a comparative study

Guangcai Zhang¹, Jiale Hou², Kun Feng³ , Chunfeng Wan^{1,*} , Liyu Xie⁴ ,
Songtao Xue^{4,5,*}, Mohammad Noori^{6,7} and Zhenghao Ding⁸

¹ Key Laboratory of Concrete and Prestressed Concrete Structures of the Ministry of Education, Southeast University, Nanjing, People's Republic of China

² Department of Civil Engineering, Tsinghua University, Beijing, People's Republic of China

³ School of Natural and Built Environment & School of Mechanical and Aerospace Engineering, Queen's University Belfast, Belfast, United Kingdom

⁴ Department of Disaster Mitigation for Structures, Tongji University, Shanghai, People's Republic of China

⁵ Department of Architecture, Tohoku Institute of Technology, Sendai, Japan

⁶ Department of Mechanical Engineering, California Polytechnic State University, San Luis Obispo, CA, United States of America

⁷ School of Civil Engineering, University of Leeds, Leeds, United Kingdom

⁸ JSPS International Research Fellow, Division of Environmental Science and Technology, Kyoto University, Kyoto, Japan

E-mail: wan@seu.edu.cn, xue@tongji.edu.cn, guangcaizhang@seu.edu.cn, hjl23@mails.tsinghua.edu.cn, k.feng@qub.ac.uk, liyuxie@tongji.edu.cn, mnoori52@yahoo.com and zhenghaoding@um.edu.mo

Received 17 September 2023, revised 1 November 2023

Accepted for publication 19 February 2024

Published 28 February 2024



CrossMark

Abstract

The identification of structural damage with the unavailability of input excitations is highly desired but challenging since structural dynamic responses are affected by the coupling effect of structural parameters and external excitations. To deal with this issue, in this paper, an output-only damage identification strategy based on swarm intelligence algorithms and correlation functions of strain responses is proposed to identify structures subjected to single or multiple unknown white noise excitations. In the proposed strategy, four different population-based optimization algorithms—particle swarm optimization, the butterfly optimization algorithm, the tree seed algorithm, and a micro search Jaya (MS-Jaya)—are employed and compared. The micro search mechanism is integrated into a basic Jaya algorithm to improve its computational efficiency and accuracy by eliminating some damage variables with small values for the identified best solution after several iterations. The objective function is established based on the proposed auto/cross-correlation function of strain responses and a penalty function. The effectiveness of the proposed method is verified with numerical studies on a simply supported beam structure and a steel grid benchmark structure under ambient excitation. In addition, the effect of the reference point, number of sensors, and arrangement of strain gauges on the performance of the proposed method are discussed in detail. The investigated results demonstrate that the proposed approach can accurately detect, locate, and

* Authors to whom any correspondence should be addressed.

quantify structural damage with limited sensors and 20% noise-polluted strain responses. In particular, the proposed MS-Jaya algorithm presents a more superior capacity in solving the optimization-based damage identification problem than the other three algorithms.

Keywords: damage identification, swarm intelligence algorithms, Jaya algorithm, strain responses, correlation function, micro search mechanism

1. Introduction

During a long-term service period, civil engineering structures may accumulate damage or even collapse since they are inevitably subjected to various loads, such as earthquakes, typhoons, floods, and the coupling effect of environmental erosion, degradation of material, and fatigue, resulting in catastrophic accidents, which necessitates continuous health monitoring, early damage identification, and timely arrangement of maintenance for existing and aging civil infrastructures [1]. Over the past three decades, considerable identification methods have been proposed and employed to detect the existence, location, and severity of structural damage. Some traditional local evaluation methods, such as Computed Tomography scanning, electromagnetic wave, and acoustic emission techniques, are time-consuming and inaccessible to the damaged area under certain circumstances, especially for large-scale and complex structures [2]. On the contrary, global vibration-based identification methods have received wide attention, achieving fruitful research results owing to the merits of easy operation, rapid identification, and non-destructive features. The basic idea of these methods is that structural dynamic responses (displacement, velocity, acceleration, strain) and modal parameters can be used to inversely identify the occurrence of early damage in a structural system [3].

Vibration-based damage identification methods can be roughly divided into frequency domain methods and time domain methods. Frequency domain methods seek to identify structural damage based on the variation of model information, such as natural frequencies [4], mode shapes [5], modal strain energy [6], mode shapes curvature [7], flexibility matrices [8], and a combination of damage indicators [9]. Nevertheless, these methods may be unreliable in the identification of damage presence, location, and severity, according to previous studies. Farrar and Doebling [10] reported that the variations of frequencies caused by structural damage were possibly less than by environmental temperature. Perry and Koh [11] found that high mode shapes were sensitive to minor damage and tend to be quite difficult to accurately obtain due to the adverse effect of measurement noise.

In consideration of the limitations of frequency domain methods, time domain methods directly using raw data recorded from sensors have been widely developed and utilized, such as least-square estimation [12], wavelet packet transform [13], particle filters [14], and response sensitivity-based methods [15]. However, most of these traditional identification methods heavily depend on good estimation of unknown parameters and appropriate gradient information of

the objective function. In addition, the absence of external excitation measurements would pose huge challenges in detecting structural damage because substantial effort is needed to reconstruct or identify unknown excitations [16]. For example, Zhu *et al* [17] simultaneously identified the input force and structural damage using a response reconstruction technique. Jayalakshmi and Rao [18] developed a novel approach for simultaneous identification of structural parameters and input forces by an improved firefly algorithm and Tikhonov regularization method. Xu *et al* [19] introduced a weighted adaptive iterative least-squares estimation method and successfully identified structural parameters and unknown excitations. However, considerable computational resources are necessarily consumed since damage identification and force identification are usually iteratively implemented. Furthermore, artificial input forces are generally required, and it may be difficult to designedly excite large-scale engineering structures such as super high-rise buildings, large-span space structures, and offshore platforms. Compared with artificial excitation, identifying structural damage using dynamic responses under ambient excitation (wind load, traffic load, wave load, etc) is more consistent with the actual service condition. Some correlation function-based damage identification methods have been developed owing to the merits of high sensitivity to structural damage but high noise immunity and unnecessary force measurement, etc [20–22]. Yang *et al* [23] constructed a cross-correlation function amplitude vector-based damage identification approach under steady random excitation. Li and Law [24] applied the covariance of the auto/cross-correlation matrix of accelerations to identify the multiple damages of a simply supported truss structure. Ni *et al* [25] presented a correlation function of an acceleration responses-based method under multiple unknown white noise excitations. On this basis, Zhang *et al* [26] introduced an adjacent acceleration correlation function and proved it to be more robust than reference point-defined methods.

Compared with accelerometers, strain gauges are cheaper and easier to install at the surface of structural elements or embed inside concrete bridge decks, dams, etc, to record strain response at inaccessible locations. Furthermore, it has been found that strain responses are highly sensitive to structural local damage [27, 28]. In other words, minor damage to structural members, holes, cracks, and reduction of a cross section can be directly reflected in the measured strain responses. Therefore, extensive attention has been drawn to the use of strain responses for damage identification. For instance, an environmental excitation incomplete strain

mode method was presented to identify the damage of space truss structures under environmental excitation based on strain data [29]. The changes of relative strain responses were used to evaluate the damage severity of fractured beams [30]. Nowadays, more strain-based damage indexes, such as strain mode shapes [31], strain frequency response function [32], strain standard deviation [33], and the correlation function amplitude vector of dynamic strain [34] have been proposed, and they provide pleasing identification results.

However, challenges still exist. Most existing strain-based methods require information on measured responses and input forces, a considerable number of sensors, and they tend to be sensitive to measurement noise, which significantly limits their practical application in real structures. How to identify damage to a structure accurately and efficiently under unknown ambient excitation with limited sensors and noise-polluted strain responses needs to be further investigated. To address this issue, a correlation function of strain responses for damage identification under single or multiple unknown white noise excitations is proposed in the present study. The proposed correlation function of strain response is a function of structural parameters. Thus, the local damage of a structural component would result in a change of the correlation function such that the damage location and extent can be inversely identified.

Mathematically, structural damage identification can be formulated as a linearly constrained multidimensional nonlinear optimization problem. To deal with this problem, a proper objective function is established by minimizing the discrepancy between the measured correlation function of the strain response from the damaged physical structure and the estimated one from the numerical model, and optimization algorithms can be applied to obtain the optimal variables by iteratively optimizing the objective function. With the development of soft computing techniques, support vector machines [35], genetic algorithms [36], evolutionary algorithms [37], k -nearest neighbors [38], etc, have been widely employed in various real-world engineering problems. In particular, swarm intelligence algorithms inspired by the collective behavior of social creatures, such as particle swarm optimization (PSO) [39], differential evolution (DE) [40], the simplified dolphin echolocation algorithm [41], the butterfly optimization algorithm (BOA) [42], the cuckoo optimization algorithm [43], and the tree seeds algorithm (TSA) [44] are increasingly being developed and applied in structural damage identification owing to their inherent advantages of powerful search capacity, loose requirement on initial value, and ease of implementation of parallel computing [45]. Zhou *et al* [46] described a hybrid butterfly optimization and DE algorithm and proved that it can achieve better performance than single algorithms. Khatir *et al* [47] utilized a teaching-learning-based optimization algorithm, and Huang *et al* [48] used an improved whale optimization algorithm to determine the locations and extent of structural damage. Although many successful applications in structural identification have been achieved,

these heuristic algorithms may still suffer from the drawback of unsatisfactory computational efficiency, especially for complex optimization problems.

A novel population-based stochastic algorithm was proposed for solving global optimization problems, named the Jaya algorithm. Different from some popular algorithms, such as PSO, DE, the BOA, etc, the Jaya algorithm has no requirement on algorithm-specific parameters [49, 50]. Since no trial-and-error procedures are required, substantial computational resources can be saved. The Jaya algorithm has been successfully applied to identify structural damage [51, 52], while extensive objective function evaluations are still needed after approaching the neighborhood of the exact value [26]. Although some measures have been taken to improve the computational efficiency and global search ability of the Jaya algorithm, it is still difficult to balance the computational resources between global and local searches. Herein, a micro search (MS) mechanism is integrated into the Jaya algorithm (MS-Jaya) by eliminating some low damage variables of the identified best solution after several iterations. In this way, the dimensions of the search space are gradually reduced, and the exact locations and extent of damaged elements can be more accurately and efficiently identified [53].

This paper proposes an output-only structural damage identification strategy based on swarm intelligence algorithms and the correlation functions of strain responses. Four different swarm intelligence algorithms, PSO, the BOA, the TSA, and MS-Jaya, are investigated for a comparison study. The correlation functions of strain responses are theoretically derived when the structure is subjected to single or multiple unknown white noise excitations. The effectiveness of the proposed output-only identification method is demonstrated by numerical studies on a simply supported beam structure and a steel grid benchmark structure. Furthermore, appropriate selection of reference points and the number of sensors are also discussed.

2. Strain cross-correlation function for damage identification

The second-order differential equation of motion for a multi-degrees-of-freedom system can be expressed as

$$M\ddot{u}(t) + C\dot{u}(t) + Ku(t) = Lf(t), \quad (1)$$

where M , C , and K stand for the mass, damping, and stiffness matrices of the structural model; $u(t)$, $\dot{u}(t)$, and $\ddot{u}(t)$ represent the vectors of displacement, velocity, and acceleration, respectively; $f(t)$ denotes the time-dependent external force applied at the structure; L is a mapping vector with the value of 1 at the excitation location and 0 at others. Rayleigh damping is adopted and a 5% modal damping ratio ξ_r is associated with the first two vibrational modes ($r = 1, 2$).

To simulate the damage to elements in the structure, herein, a popular model is used by reducing the elemental stiffness.

A series of scalar variables $\alpha = (\alpha_1, \alpha_2, \dots, \alpha_i, \dots, \alpha_{ne})$ taken from the range of $[0, 1]$ are introduced as follows:

$$K_d = \sum_{i=1}^{ne} (1 - \alpha_i) K_i^e, 0 \leq \alpha_i \leq 1, \quad (2)$$

where K_d denotes the global stiffness matrix of the damaged structure; K_i^e means the i th elemental stiffness; ne represents the number of elements; and α_i is the damage index corresponding to the i th elemental stiffness. $\alpha_i = 0$ means the i th element is intact while $\alpha_i = 1$ indicates this element is completely damaged.

According to the displacement–strain relation, strain responses at location p with local coordinates (x, y) in a typical Euler beam element e can be calculated by [54]

$$\begin{aligned} \varepsilon_p = & \frac{u_j^* - u_i^*}{l} + \left(\frac{6y}{l^2} - \frac{12xy}{l^3} \right) v_i^* + \left(\frac{4y}{l} - \frac{6xy}{l^2} \right) \theta_i^* \\ & + \left(-\frac{6y}{l^2} + \frac{12xy}{l^3} \right) v_j^* + \left(\frac{2y}{l} - \frac{6xy}{l^2} \right) \theta_j^*, \end{aligned} \quad (3)$$

where $[u_i^*, v_i^*, \theta_i^*, u_j^*, v_j^*, \theta_j^*]^T$ stands for the two nodal displacement vectors of element e ; l is the length of elements; and $y = h_t/2$, h_t is the height of the element.

2.1. Single white noise excitation

If the system has zero initial conditions, the strain response of location p under external excitation $f(t)$ can be expressed as

$$\varepsilon_p(t) = \int_{-\infty}^t h_p^\varepsilon(t - \tau) f(\tau) d\tau, \quad (4)$$

where h_p^ε stands for the strain unit impulse response function of location p ; $\varepsilon_p(t)$ means the strain response at time t .

The strain unit impulse response function $h_p^\varepsilon(t)$ of location p with coordinates (x, y) can be computed with the displacement unit impulse response function according to the relationship of equation (3), as follows:

$$\begin{aligned} h_p^\varepsilon(t) = & \frac{h_{e4}(t) - h_{e1}(t)}{l} + \left(\frac{6y}{l^2} - \frac{12xy}{l^3} \right) h_{e2}(t) + \left(\frac{4y}{l} - \frac{6xy}{l^2} \right) \\ & \times h_{e3}(t) + \left(-\frac{6y}{l^2} + \frac{12xy}{l^3} \right) h_{e5}(t) + \left(\frac{2y}{l} - \frac{6xy}{l^2} \right) h_{e6}(t), \end{aligned} \quad (5)$$

where $h_{e1}(t), h_{e2}(t), h_{e3}(t), h_{e4}(t), h_{e5}(t), h_{e6}(t)$ represent the displacement unit impulse response functions for the degrees-of-freedom $e1, e2, e3, e4, e5$, and $e6$, respectively.

Assuming that the initial system is in static equilibrium, the displacement unit impulse response functions can be obtained by the following Newmark method [25]:

$$\begin{cases} M\ddot{h}(t) + C\dot{h}(t) + Kh(t) = 0 \\ h(0) = 0, \dot{h}(0) = M^{-1}L \end{cases}, \quad (6)$$

where $h(t)$, $\dot{h}(t)$, and $\ddot{h}(t)$ stand for the unit impulse displacement, velocity, and acceleration vectors, respectively.

The cross-correlation function of strain responses at the p th and q th measurements of the system under single excitation can be formulated as

$$\begin{aligned} R_{pq}^\varepsilon(\tau) = E[\varepsilon_p(t) \varepsilon_q(t + \tau)] = E \left\{ \int_{-\infty}^t h_p^\varepsilon(t - \sigma_1) f(\sigma_1) d\sigma_1 \right. \\ \left. \times \int_{-\infty}^{t+\tau} h_q^\varepsilon(t + \tau - \sigma_2) f(\sigma_2) d\sigma_2 \right\}, \end{aligned} \quad (7)$$

where σ_1 and σ_2 denote the small time interval.

The correlation function $f(\sigma_1)$ and $f(\sigma_2)$ can be calculated by the following equation when the ambient excitation is assumed to be the white noise excitation [25]:

$$E(f(\sigma_1)f(\sigma_2)) = S\delta(\sigma_1 - \sigma_2), \quad (8)$$

where S stands for a constant, which defines the magnitude of excitation $f(t)$ when $\sigma_1 = \sigma_2$; δ means the Dirac delta function.

Substituting equation (8) into equation (7) with $\int_0^\infty \delta(\tau) d\tau = 1$, according to the property of the Dirac delta function, the cross-correlation function of strain responses is simplified as [25]

$$R_{pq}^\varepsilon(\tau) = S \int_0^{+\infty} h_p^\varepsilon(t) h_q^\varepsilon(t + \tau) dt = H^\varepsilon(\theta) S, \quad (9)$$

where $H^\varepsilon(\theta) = \int_0^{+\infty} h_p^\varepsilon(t) h_q^\varepsilon(t + \tau) dt$. From equation (9), the cross-correlation function of strain responses $R_{pq}^\varepsilon(\tau)$ only depends on structural parameters θ to be identified and a constant S related to the input force.

The constant coefficient S can be estimated by [25]

$$S_{\text{est}} = (H_{\text{est}}^{\varepsilon T} H_{\text{est}}^\varepsilon)^{-1} H_{\text{est}}^{\varepsilon T} R_{\text{mea}}^\varepsilon, \quad (10)$$

where $H_{\text{est}}^\varepsilon$ denotes the estimated convolution of the strain unit impulse response functions; $R_{\text{mea}}^\varepsilon$ is the measured cross-correlation function of strain responses.

If the strain response at the γ th measurement is selected as the reference point, the auto/cross-correlation function R^ε is written as

$$R^\varepsilon = [R_{\gamma,1}^\varepsilon, R_{\gamma,2}^\varepsilon, \dots, R_{\gamma,\gamma}^\varepsilon, \dots, R_{\gamma,n}^\varepsilon]^T, \quad (11)$$

where γ is the reference point; n means the number of strain responses.

2.2. Multiple white noise excitations

Structures may be subjected to external excitation at multiple points, so a more complex but practical case of multiple white noise excitations is considered. The response of a linear structural system under multi-point external excitations is equal to the superposition of those under single excitation. The strain response at location p can be expressed as

$$\varepsilon_p(t) = \varepsilon_{p,1}(t) + \varepsilon_{p,2}(t) + \dots + \varepsilon_{p,nf}(t) = \sum_{\mu=1}^{nf} \varepsilon_{p,\mu}(t), \quad (12)$$

where $\varepsilon_{p,\mu}(t)$ stands for the strain response at location p under the μ th single excitation; nf denotes the number of forces.

The cross-correlation function of strain responses at the p th and q th measurements of the system under multiple excitations can be formulated as [25]

$$\begin{aligned} R_{\varepsilon_p, \varepsilon_q}(\tau) &= R_{(\varepsilon_{p,1} + \varepsilon_{p,2} + \dots + \varepsilon_{p,nf}), (\varepsilon_{q,1} + \varepsilon_{q,2} + \dots + \varepsilon_{q,nf})}(\tau) \\ &= \sum_{\mu=1}^{nf} \sum_{\varsigma=1}^{nf} R_{\varepsilon_{p,\mu}, \varepsilon_{q,\varsigma}}(\tau), \end{aligned} \quad (13)$$

where μ and ς represent the locations of external excitation.

$$\begin{aligned} R_{\varepsilon_{p,\mu}, \varepsilon_{q,\varsigma}}(\tau) &= \int_{-\infty}^t \int_{-\infty}^{t+\tau} h_{p,\mu}^\varepsilon(t - \sigma_1) h_{q,\varsigma}^\varepsilon(t + \tau - \sigma_2) \\ &\quad \times E(f_\mu(\sigma_1) f_\varsigma(\sigma_2)) d\sigma_1 d\sigma_2, \end{aligned} \quad (14)$$

where $E(f_\mu(\sigma_1) f_\varsigma(\sigma_2)) = 0$ for $\mu \neq \varsigma$; $E(f_\mu(\sigma_1) f_\varsigma(\sigma_2)) = S_\mu \delta(\mu_1 - \mu_2)$ for $\mu = \varsigma$. Thus, equation (13) can be simplified as [25]

$$\begin{aligned} R_{\varepsilon_p, \varepsilon_q}(\tau) &= \sum_{\mu=1}^{nf} R_{\varepsilon_{p,\mu}, \varepsilon_{q,\mu}}(\tau) \\ &= \sum_{\mu=1}^{nf} \left(S_\mu \int_0^{+\infty} h_{p,\mu}^\varepsilon(t) h_{q,\mu}^\varepsilon(t + \tau) dt \right), \end{aligned} \quad (15)$$

where S_μ represents a constant associated with the μ th excitation,

$$H_\mu^\varepsilon(\theta) = \int_0^{+\infty} h_{p,\mu}^\varepsilon(t) h_{q,\mu}^\varepsilon(t + \tau) dt, \quad (16)$$

where $H_\mu^\varepsilon(\theta)$ is the convolution of strain unit impulse response functions for h_p^ε and h_q^ε under the μ th single excitation,

$$\begin{aligned} R_{\varepsilon_p, \varepsilon_q}(\tau) &= [H_1^\varepsilon, H_2^\varepsilon, H_\mu^\varepsilon, \dots, H_{nf}^\varepsilon] \\ &\quad \times [S_1, S_2, \dots, S_\mu, \dots, S_{nf}]^T = H^\varepsilon(\theta) S. \end{aligned} \quad (17)$$

Equation (17) shows that the cross-correlation function of strain responses can be expressed as two parts: the first part, $H^\varepsilon(\theta)$, is the function of unknown structural parameters θ , and the second part, S , is a constant vector associated with the energy of the external excitations.

3. Identification methods

3.1. PSO algorithm

PSO is a typical representative of a swarm intelligence optimization algorithm, originally proposed by Eberhart and Kennedy in 1995 [55]. PSO is inspired by the foraging behaviors of birds to find the optimal solution through collaboration and information sharing among individuals in the group.

In PSO, the current location and flight process of a particle can be considered as a potential candidate for the corresponding optimization problem and the searching process for a solution, respectively. In the process of foraging, each particle has two attributes: velocity and position, where velocity represents the speed of movement and position means the direction of movement. The velocity and position of the i th particle in the G -iteration can be dynamically adjusted according to the best solution of individual particles P_{best}^G and the best-so-far solution of the entire population g_{best}^G , as follows:

$$V_i^{G+1} = \omega V_i^G + c_1 r_1 (P_{\text{best}}^G - X_i^G) + c_2 r_2 (g_{\text{best}}^G - X_i^G) \quad (18)$$

$$X_i^{G+1} = X_i^G + V_i^{G+1}, \quad (19)$$

where V_i and X_i represent the current velocity and position of the i th particle, respectively; ω stands for the inertia weight, and it linearly decreases from 0.9 to 0.4; r_1 and r_2 are two random numbers in the range of $[0, 1]$; c_1 and c_2 mean the cognitive and social scaling parameters, respectively.

Finally, repeat the iteration until the convergence tolerance or the maximum number of iterations is satisfied.

3.2. BOA

The BOA is a nature-inspired swarm intelligence algorithm proposed by Arora and Singh in 2019 [56]. It mimics the foraging and mating behaviors of biological butterflies in nature using sense of smell to determine the location of food or mating objects. Nowadays, the BOA has been widely used to deal with various real-world optimization problems owing to its novel concept, simple structure, and easy operation. In the BOA, it is assumed that butterflies can generate different intensities of fragrance, which is associated with their objective value, as follows:

$$\varphi_i = cI^a, \quad (20)$$

where φ_i represents the magnitude of the fragrance perceived by the i th butterfly; c means the sensory modality taken from the range of $[0, 1]$; I denotes the stimulus intensity, correlated with the objective function value; and a stands for the power exponent within the range of $[0, 1]$.

There are two different search phases in the iteration process of the BOA. When a butterfly is attracted by the best butterfly who emits the most fragrance among the population, it will move toward the best butterfly, called the local search phase. A butterfly will perform a random walk if it cannot sense the fragrance emitted by any other butterfly in the population, called the global search phase. The equations of the global exploration phase and local exploitation phase are mathematically formulated as equations (21) and (22), respectively:

$$X_i^{G+1} = X_i^G + (r^2 \times X_j^G - X_k^G) \times \varphi_i \quad (21)$$

$$X_i^{G+1} = X_i^G + (r^2 \times X_{\text{best}}^G - X_i^G) \times \varphi_i, \quad (22)$$

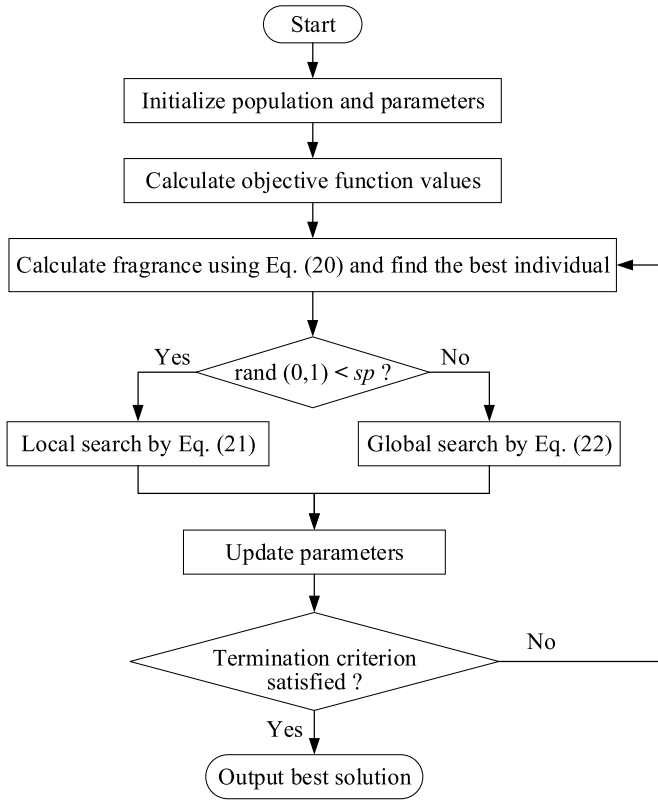


Figure 1. Flowchart of the BOA.

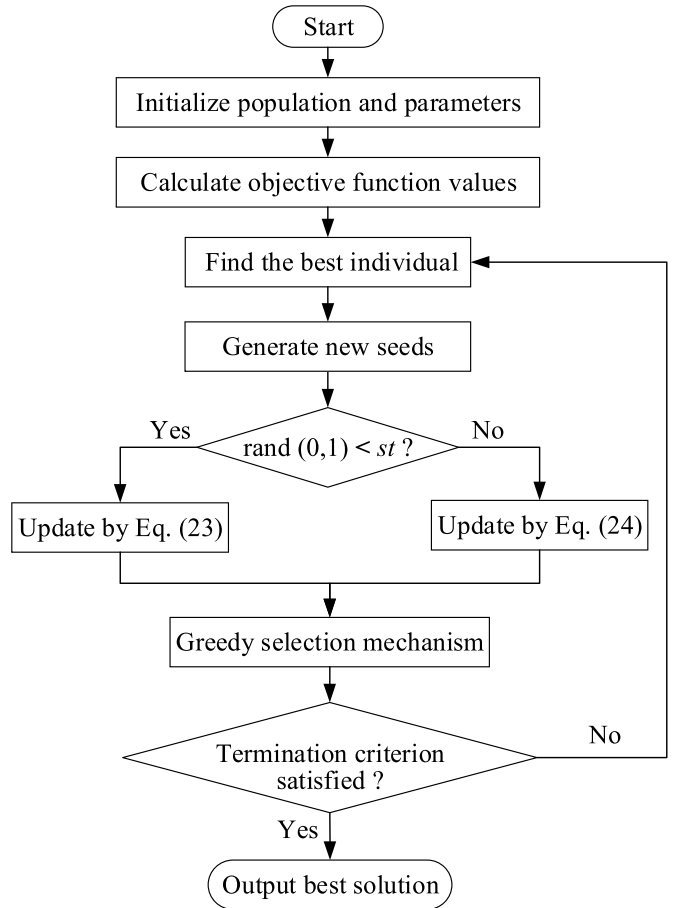


Figure 2. Flowchart of the TSA.

where X_i^G and X_i^{G+1} stand for the i th butterfly in the G and $(G + 1)$ iteration; r means a random number of the interval of $[0, 1]$; X_j^G and X_k^G are two different butterflies randomly selected from the population; and X_{best}^G represents the best-so-far solution in the current iteration.

Another parameter, the switch probability, sp , is introduced to determine whether a global or local search will be conducted. A flowchart of the BOA is shown in figure 1.

3.3. TSA

The TSA is a novel heuristic algorithm proposed by Kiran in 2015 to solve continuous optimization problems [57], inspired by the relationships between trees and their seeds in nature. In the TSA, the location of trees and seeds can be considered a feasible solution to the optimization problem, and the surface of these trees is viewed as a search space for the optimization issue. The algorithm utilizes two different search equations to generate new seeds, as follows:

$$Seed_{i,j} = T_{i,j} + \beta_{i,j} \times (B_j - T_{k,j}) \quad (23)$$

$$Seed_{i,j} = T_{i,j} + \beta_{i,j} \times (T_{i,j} - T_{k,j}), \quad (24)$$

where $Seed_{i,j}$ is the j th dimension of the i th seed produced by i th tree; $T_{i,j}$ is the j th dimension of the i th tree; B_j is the j th dimension of the best-so-far tree position; $T_{k,j}$ is the j th dimension of the k th tree randomly selected from the current population; and $\beta_{i,j}$ is the scaling factor randomly generated within the range of $[-1, 1]$.

In order to balance the trade-off between the local and global search, switch tendency, st , is introduced in the TSA. If a randomly produced number within the range of $[0, 1]$ is lower than st , equation (23) is used to update the dimension of the seed, otherwise equation (24) is implemented. After seeds are generated for a tree, the best one is selected and compared with the tree. If the seed is better than the current tree, the seed would substitute for this tree. A more detailed introduction of the TSA can be found in [57]. A flowchart of the TSA is presented in figure 2.

3.4. MS-Jaya algorithm

The Jaya algorithm is a novel global search population-based algorithm proposed by Rao for solving diverse constrained and unconstrained optimization problems. The basic concept of the Jaya algorithm is that the offspring of a population would move toward the optimal solution and meanwhile move away from the inferior solution. After initializing the population in predefined search space limits X_1, X_2, \dots, X_{np} , objective functions for each candidate solution are evaluated and ranked. Then, the best solution X_{best} and the worst X_{worse} are determined. The updating equation of offspring is performed as follows:

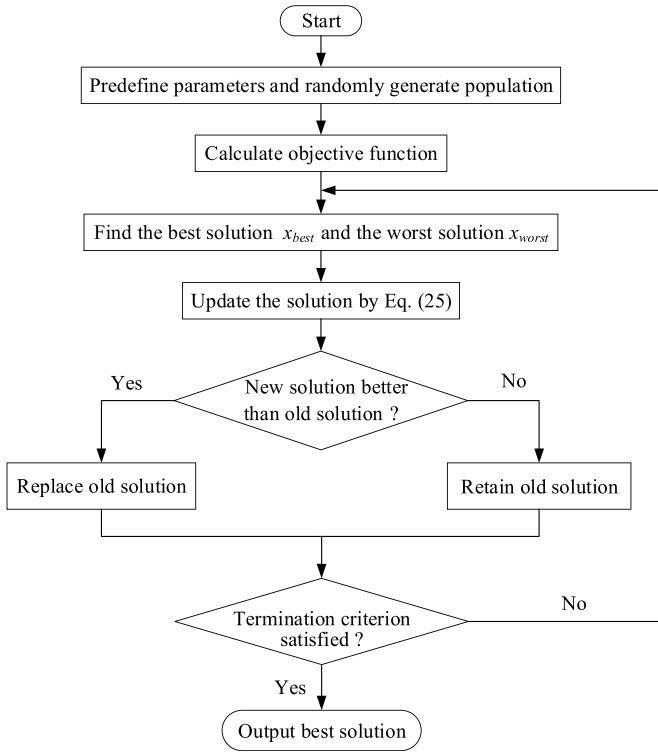


Figure 3. Flowchart of the Jaya algorithm.

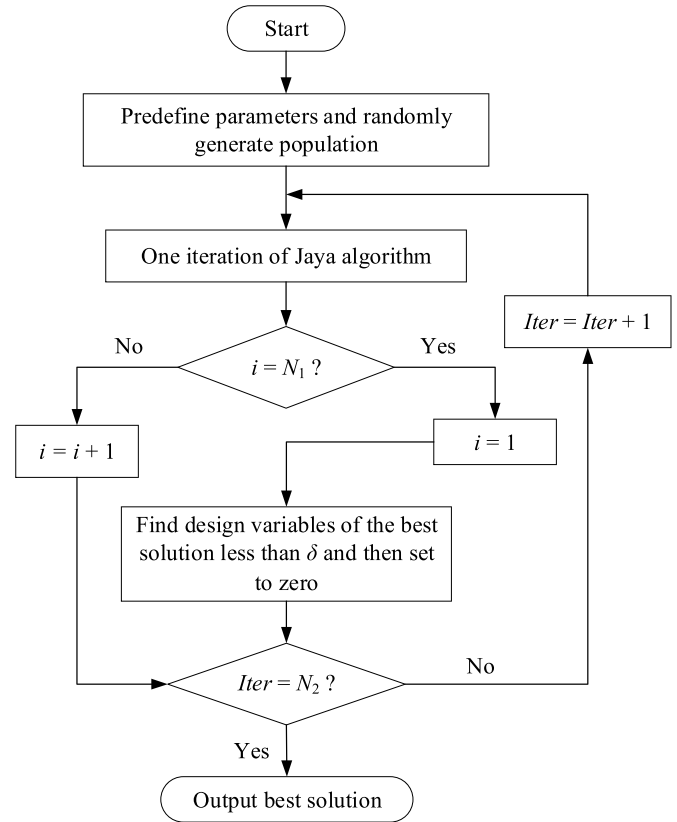


Figure 4. Flowchart of the MS-Jaya algorithm.

$$U_{i,j}^G = X_{i,j}^G + rand_1 \times (X_{best,j}^G - |X_{i,j}^G|) - rand_2 \times (X_{worst,j}^G - |X_{i,j}^G|), \quad (25)$$

where $X_{i,j}^G$ represents the j th variable of the i th candidate solution at the G th iteration; $U_{i,j}^G$ is the updated value of $X_{i,j}^G$; $X_{best,j}^G$ and $X_{worst,j}^G$ stand for the j th variable of the best candidate and worst candidate, respectively; and $rand_1$ and $rand_2$ mean a random number within the range of $[0, 1]$.

On the right-hand side of equation (25), the second term indicates the tendency of candidates to move toward the best solution while the third term represents the tendency to avoid the worst solution. Subsequently, greedy selection is implemented to ensure that the solution with a better objective value survives to the next iteration:

$$X_{i,G+1} = \begin{cases} U_{i,G} & \text{if } f(U_{i,G}) < f(X_{i,G}) \\ X_{i,G} & \text{otherwise} \end{cases}, \quad (26)$$

where $f(U_{i,G})$ and $f(X_{i,G})$ stand for the objective values of the new solution $U_{i,G}$ and the previous solution $X_{i,G}$, respectively.

The final identified optimal solution will be output when the termination criterion is satisfied. A flowchart of the Jaya algorithm is presented in figure 3. It is found that, different from PSO, the BOA, and the TSA, the Jaya algorithm does not need any algorithm-specific parameters.

Although the Jaya algorithm has been successfully employed to solve optimization-based structural damage identification problems, it may still suffer from the drawbacks of unfavorable accuracy, slow speed, or premature convergence to local optima, especially for large-scale and

complex structural systems. To deal with this issue, in this study, an MS mechanism is integrated into the Jaya algorithm to try to reduce the dimensions of unknown parameters to be identified during the search process. The proposed MS-Jaya algorithm is capable of improving damage identification accuracy and computational efficiency by eliminating some damage variables with small values for the best solution after several iterations because of reducing the time spent on exploring far outside the neighborhood where the optimal solution lies.

It should be noted that the number of damaged elements is generally much less than the number of healthy elements. The identified best individual tends to approximate the actual damage situation after a certain number of iterations of the Jaya algorithm. In this case, the identified variables of the best solution with damage extent lower than the maximum damage limit δ_{max} can be set as zero and considered as intact elements, which is able to obviously reduce the dimension of the search space:

$$\alpha_i = 0, \text{ if } \alpha_i < \delta_{max}. \quad (27)$$

Figure 4 presents a detailed flowchart of the proposed MS-Jaya algorithm. In this algorithm, N_1 and N_2 stand for the number of iterations to implement the MS mechanism and the maximum iteration number, respectively.

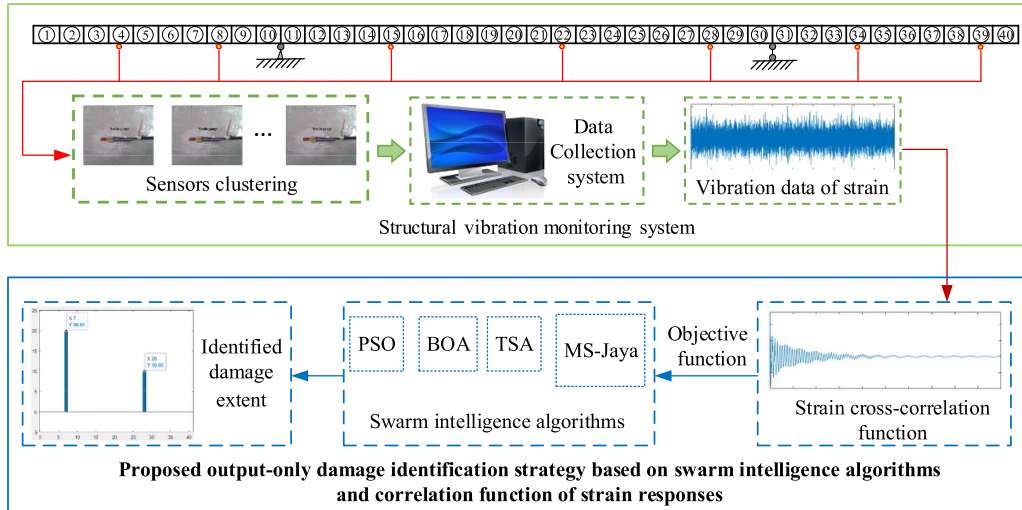


Figure 5. The workflow of the proposed output-only damage identification approach.

3.5. Identification procedures

An output-only damage identification method based on strain correlation function with swarm intelligence algorithms, i.e. PSO, the BOA, the TSA, and MS-Jaya, is presented. The workflow of the proposed identification method is revealed in figure 5.

The implementation procedures are introduced as follows:

Step 1: measure the dynamic strain responses of the damaged structure with preinstalled sensors under single or multiple ambient excitations and then calculate the measured correlation function $\mathbf{R}_{\text{mea}}^\varepsilon$ with recorded strain responses and selected reference points.

Step 2: define algorithm parameters and randomly generate initial values of damage variables to be identified within the upper and lower search space limits for PSO, the BOA, the TSA, and MS-Jaya.

Step 3: for each individual θ^i in the population, calculate $H_{\text{est}}^\varepsilon(\theta^i)$ and the constant vector S_{est} with the equations of $H_{\text{est}}^\varepsilon(\theta) = \int_0^{+\infty} h_p^\varepsilon(t) h_q^\varepsilon(t + \tau) dt$ and $S_{\text{est}} = (\mathbf{H}_{\text{est}}^\varepsilon T \mathbf{H}_{\text{est}}^\varepsilon)^{-1} \mathbf{H}_{\text{est}}^\varepsilon T \mathbf{R}_{\text{mea}}^\varepsilon$ under single or multiple white noise excitations, and then compute the estimated correlation function $R_{\text{est}}^\varepsilon(\theta^i) = H_{\text{est}}^\varepsilon(\theta^i) S_{\text{est}}$.

Step 4: evaluate the objective function f_{obj} for each candidate by minimizing the difference between the measured and estimated cross-correlation function of strain response, as follows:

$$f_{\text{obj}} = \frac{1}{c + \lambda(\theta^i) \left(\frac{\|R_{\text{mea}}^\varepsilon - R_{\text{est}}^\varepsilon(\theta^i)\|^2}{\|R_{\text{mea}}^\varepsilon\|^2} \right)}, \quad (28)$$

where $\lambda(\theta^i)$ is a penalty function, related to the ratio of the number of damaged elements nd in the individual θ^i to the total number of elements ne , expressed as $\lambda(\theta^i) = (1 + \frac{nd(\theta^i)}{ne})$, which is beneficial to alleviate false alarm detection; c is a small constant, set as 0.001, so the maximum objective function value is 1000 when $R_{\text{mea}}^\varepsilon$ is equal to $R_{\text{est}}^\varepsilon$.

Step 5: generate the next candidate using four different swarm intelligence algorithms.

Step 6: repeat steps 3–5 until the predefined maximum iteration number Max_Iter is reached or the following convergence criterion is fulfilled:

$$error = \frac{\sum_{i=1}^N \frac{|K_i^{\text{iter}} - K_i^{\text{iter}-1}|}{K_i^{\text{iter}}}}{N} \leq Tol, \quad (29)$$

where N means the dimension of the parameters to identify; $K_i^{\text{iter}-1}$ and K_i^{iter} stand for the identified i th candidate solution after $(iter-1)$ and $iter$ iterations, respectively, and Tol represents the convergence tolerance, $Tol = 10^{-5}$. Finally, output the identified structural damage location and extent.

4. Numerical studies

To verify the effectiveness of the proposed damage identification approach based on swarm intelligence algorithms and the correlation function of strain responses, a simply supported beam structure is employed as a numerical example in this section. Appropriate parameter settings of four algorithms, i.e. PSO, the BOA, the TSA, and MS-Jaya, are listed in table 1. Algorithm-specific parameters of PSO, the BOA, and the TSA are recommended by [56, 58] and [44], respectively. The average values from 20 independent runs are compared for these four swarm intelligence algorithms to ensure the reliability and fairness of the identified results.

As presented in figure 6, a 16-element simply supported beam structure is utilized. The length, width, and section thickness are 1600 mm, 50 mm, and 3 mm, respectively. The simply supported beam is modeled with 17 nodes and 16 identical beam elements, and the length of each element is 100 mm. Each intermediate node has two degrees of freedom, namely,

Table 1. Parameters of PSO, the BOA, the TSA, and MS-Jaya for the simply supported beam.

Parameters	PSO	BOA	TSA	MS-Jaya
Population size np	100	100	100	100
Generations G_m	400	400	400	60
Inertia weight w	Linearly decreases from 0.9 to 0.4			
Cognitive parameter $c1$	2			
Social parameter $c2$	2			
Sensor modality c		0.01		
Power exponent a		0.1		
Switch probability sp		0.8		
Search tendency st			0.4	
N_1 of micro search				20
Damage limit δ_{max}				0.02
Total evaluations	40 000	40 000	40 000	6000

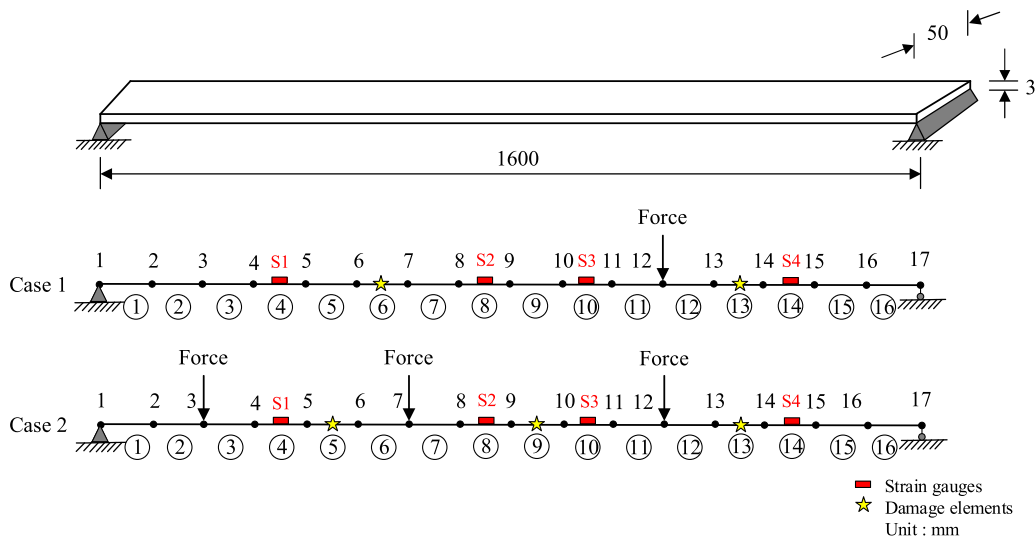


Figure 6. Numerical model of the 16-element simply supported beam structure.

a vertical translation and a rotation. For the boundary nodes, node 1 is modeled as a pin support and node 17 is modeled as a roller support. The mass density and initial elasticity modulus for the intact steel beam structure are 7860 kg m^{-3} and $2.1 \times 10^{11} \text{ N m}^{-2}$, respectively. As shown in figure 6, four strain gauges are installed at the midpoint of elements 4, 8, 10, and 14 along the upper surface of the beam to obtain the longitudinal strain responses with the sampling frequency of 500 Hz and sampling duration of 1800 s. Two different damage cases, i.e. case 1 and case 2, are studied in order to consider single and multiple ambient excitations, respectively. As listed in table 2, in case 1, we assume there is a 20% and 15% reduction in Young’s modulus at the sixth and 13th elements, namely, $\alpha_6 = 0.2$ and $\alpha_{13} = 0.15$. In damage case 2, we assume there is a 20%, 10%, and 20% reduction of stiffness in the fifth, ninth, and 13th elements, namely, $\alpha_5 = 0.2, \alpha_9 = 0.10, \alpha_{13} = 0.20$. The reason for setting different reductions of stiffness for damage case 1 and damage case 2 is to validate the effectiveness of the proposed approach by considering more damage cases.

Table 2. Damage cases under single and multiple excitations.

Damage case 1		Damage case 2	
Element no.	Damage extent	Element no.	Damage extent
6	20%	5	20%
13	15%	9	10%
		13	20%

4.1. Single excitation case

White noise is employed to simulate the ambient excitation applied at node 12 of the simply supported beam structure. In order to investigate the effect of noise on the performance of the proposed identification method, the clean strain response $\varepsilon_{clean}(t)$ is deliberately contaminated by Gaussian white noise to simulate a noise-polluted response, as follows:

$$\varepsilon_{mea} = \varepsilon_{clean} + Noise \times NI \times \text{std}(\varepsilon_{clean}), \quad (30)$$

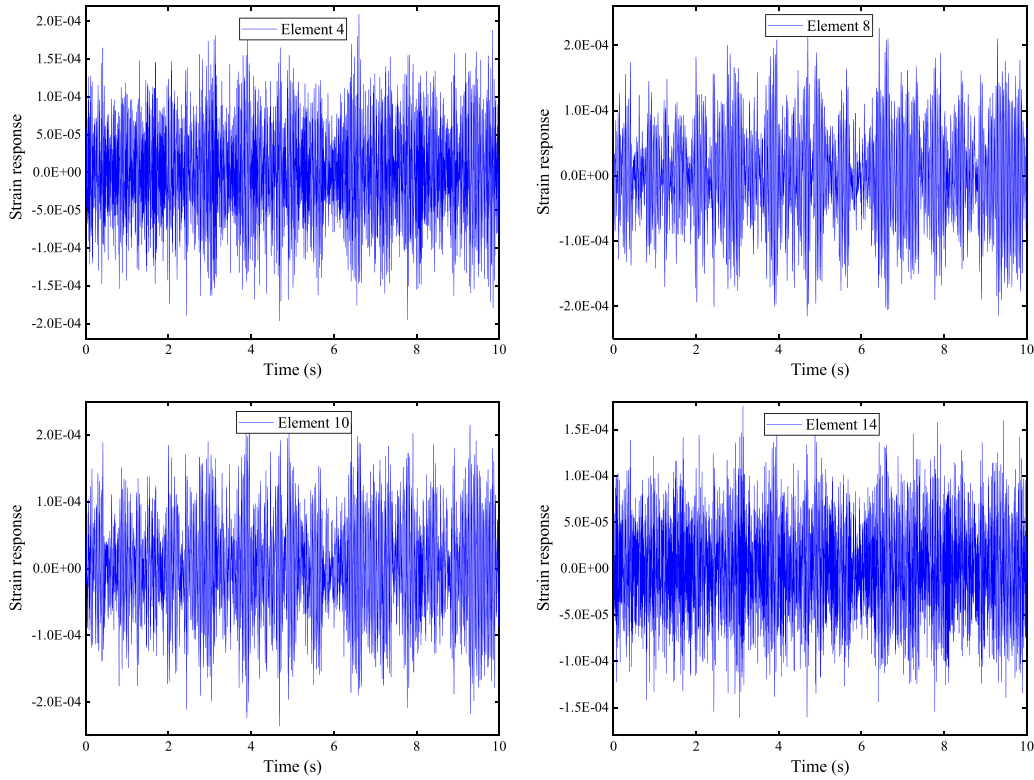


Figure 7. The strain response curves for damage case 1 (first 10 s).

where ε_{mea} means the noise-contaminated response; $Noise$ represents a Gaussian distribution noise vector with zero mean and unit standard deviation; $\text{std}(\varepsilon_{\text{clean}})$ stands for the standard deviation of the clean strain measurement; Nl denotes the percentage noise level. Three noise levels, 0%, 10%, and 20%, are considered in this numerical study. The strain response curves from four strain gauges for damage case 1 are presented in figure 7.

There are 16 unknown parameters $\alpha = (\alpha_1, \alpha_2, \dots, \alpha_i, \dots, \alpha_{16})$ to be identified with four strain responses. If the strain response at element 10 is selected as the reference point, the auto/cross-correlations function is $R = [R_{10,4}, R_{10,8}, R_{10,10}, R_{10,14}]^T$. The final damage extent and identification errors of the simply supported beam structure using the proposed four methods under 0%, 10%, and 20% noise are presented in figure 8 and table 3, respectively.

It is easily observed from figure 8 that the proposed four methods are able to successfully identify structural damage, especially for the MS-Jaya algorithm, providing the best performance with the least mean errors of only 0.41% for the noise-free case. In table 3, the damage variables of the simply supported beam are accurately identified by PSO, the BOA, the TSA, and MS-Jaya with results of less than 1.5% mean error and 6% maximum error under 10% noise, and the corresponding errors are less than 2.0% and 7.5% under 20% noise, which implies that the proposed strain correlation function-based damage identification method is insensitive to measurement noise.

In addition, the computational efficiency of the proposed four identification methods is further investigated. The convergence history of the objective function and the consumed computational times for PSO, the BOA, the TSA, and MS-Jaya are presented in figure 9 and table 4, respectively. It can be easily observed from figure 9 that the MS-Jaya algorithm achieves a smaller value of objective function, with only 60 maximum iterations, than PSO, the BOA, and the TSA. As shown in table 4, the calculated objective values of PSO, the BOA, the TSA, and MS-Jaya are 931.52, 902.24, 942.18, and 944.77, respectively. Meanwhile, the total computational time needed to run the proposed MS-Jaya algorithm is 320 s, much shorter than the 2124 s, 2088 s, and 2132 s required by PSO, the BOA, and the TSA, which indicates that the MS-Jaya algorithm can provide better identified results with less computational time than the other three methods.

Herein, the more detailed damage identification process of the proposed MS-Jaya algorithm is further presented in table 5. If the identified variables of the best solution after each 20 iterations of the Jaya algorithm are smaller than the predefined damage limit of 2%, the damage extent will be set to zero. There are five damaged elements after 20 iterations, three damaged elements after 40 iterations, and two damaged elements after 60 iterations. The final identified damage locations and extents of elements 6 and 13 agree well with the true value. As listed in table 6, the MS mechanism significantly reduces the number of suspected damaged elements after each N_1 iterations of the Jaya algorithm, which implies that integrating the

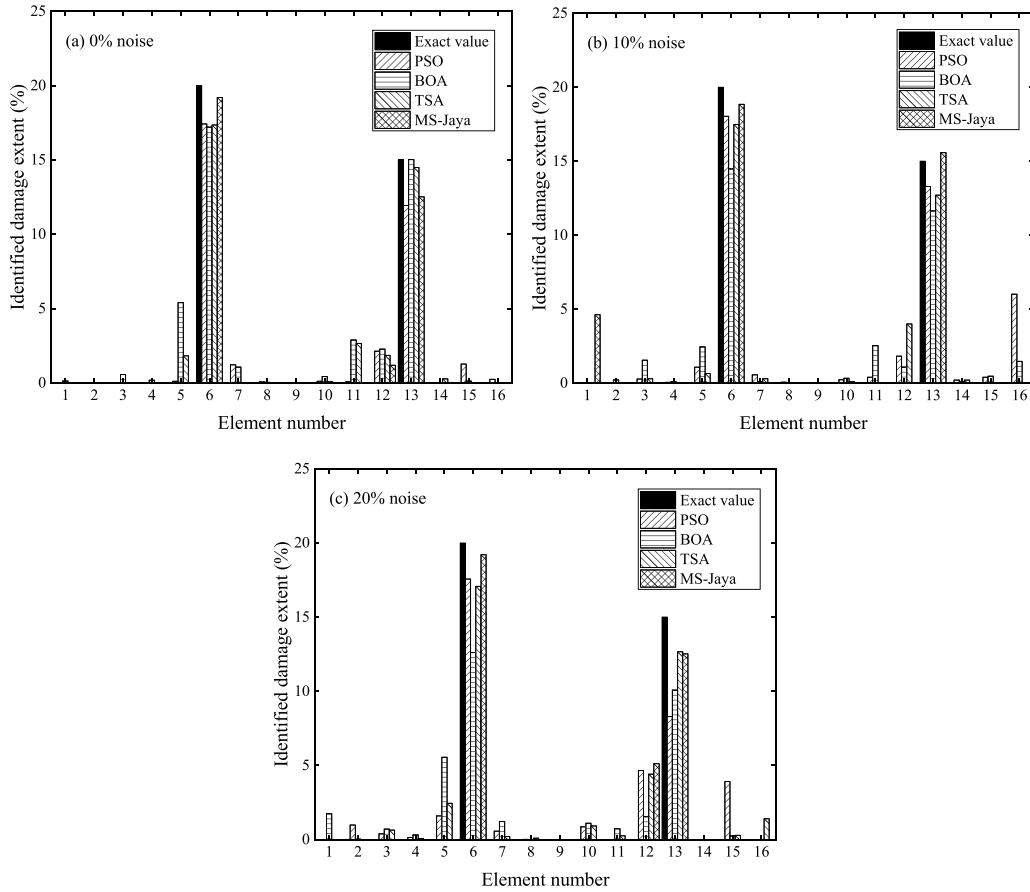


Figure 8. Identified damage extent for case 1 under single excitation: (a) 0% noise; (b) 10% noise; (c) 20% noise.

Table 3. Mean and maximum errors for damage case 1 under single excitation (%).

Methods	0% noise		10% noise		20% noise	
	Mean error	Max error	Mean error	Max error	Mean error	Max error
PSO	0.68	3.06	0.92	6.00	1.71	6.71
BOA	1.26	5.40	1.46	5.51	1.94	7.39
TSA	0.74	2.65	0.85	4.00	1.20	4.42
MS-Jaya	0.41	2.48	0.65	4.62	0.79	5.11

MS mechanism is highly effective in the identification of damage existence, location, and severity by successively eliminating the intact elements during the iteration process.

In terms of identification accuracy and computational efficiency, it can be concluded from the above studies that the proposed methods based on the swarm intelligence algorithms PSO, the BOA, the TSA, and MS-Jaya, and the cross-correlation function of strain responses can accurately and effectively identify structural damage, especially for the MS-Jaya algorithm, even with partial output-only strain responses and 20% noise-contaminated measurements.

4.2. Multiple excitations case

Three white noise excitations are applied at node 3, 7, and 12 of the simply supported beam structure. The strain

response curves from four strain gauges for damage case 2 are presented in figure 10. The measurement at the 10th element is treated as the reference point, resulting in four sets of the auto/cross-correlation function $R = [R_{10,4}, R_{10,8}, R_{10,10}, R_{10,14}]^T$. The identified results based on the swarm intelligence algorithms PSO, the BOA, the TSA, and MS-Jaya, and the correlation function of strain responses with 0%, 10%, and 20% noise are presented in figure 11, and the identified mean and maximum errors are listed in table 7.

For the noise-free case, it can be seen from figure 11 that pleasing identification results are obtained with the proposed four methods. For the worst case, the maximum error and mean error by the BOA are less than 4.5% and 2.5%. When contaminated with 10% and 20% noise, as shown in table 7, more than 6% maximum errors are achieved by PSO and the BOA, while the TSA and MS-Jaya can give more accurate identification

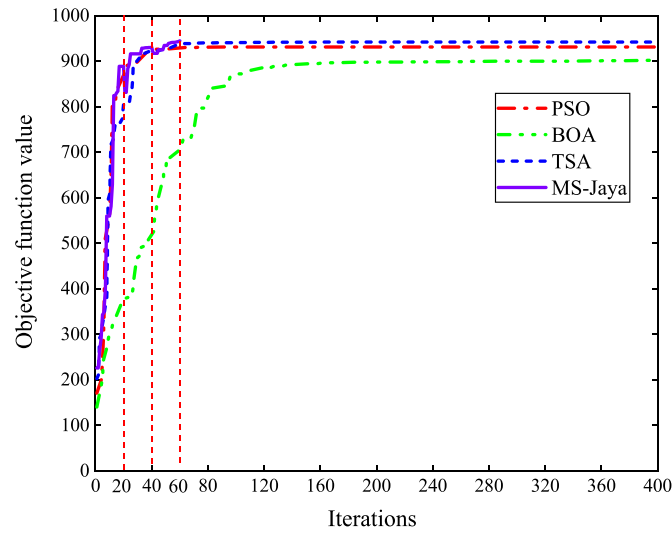


Figure 9. Convergence study for the proposed four methods in damage case 1 (0% noise).

Table 4. Comparison of computational time for PSO, the BOA, the TSA, and MS-Jaya in damage case 1.

Methods	Objective value	Number of iterations	Computational time for single iteration (s)	Total time (s)
PSO	931.52	400	5.31	2124
BOA	902.24	400	5.22	2088
TSA	942.18	400	5.33	2132
MS-Jaya	944.77	60	5.32	320

Table 5. The identified damage variables after each N_1 iterations of the Jaya algorithm (%).

Element numbers	$N_1 = 20$ iterations	$2N_1 = 40$ iterations	$3N_1 = 60$ iterations
1	0	0	0
2	0	0	0
3	0	0	0
4	0	0	0
5	0	0	0
6	12.33	19.43	19.21
7	0	0	0
8	0	0	0
9	0	0	0
10	0	0	0
11	6.93	0	0
12	14.14	4.79	0
13	10.61	12.90	12.52
14	0	0	0
15	0	0	0
16	4.12	0	0

Table 6. The number of intact and damaged elements after implementing the MS mechanism.

Iterations	0% noise		10% noise		20% noise	
	Intact	Damaged	Intact	Damaged	Intact	Damaged
1	1	15	0	16	0	16
$N_1 = 20$	11	5	9	7	8	8
$2N_1 = 40$	13	3	12	4	12	4
$3N_1 = 60$	14	2	13	3	13	3

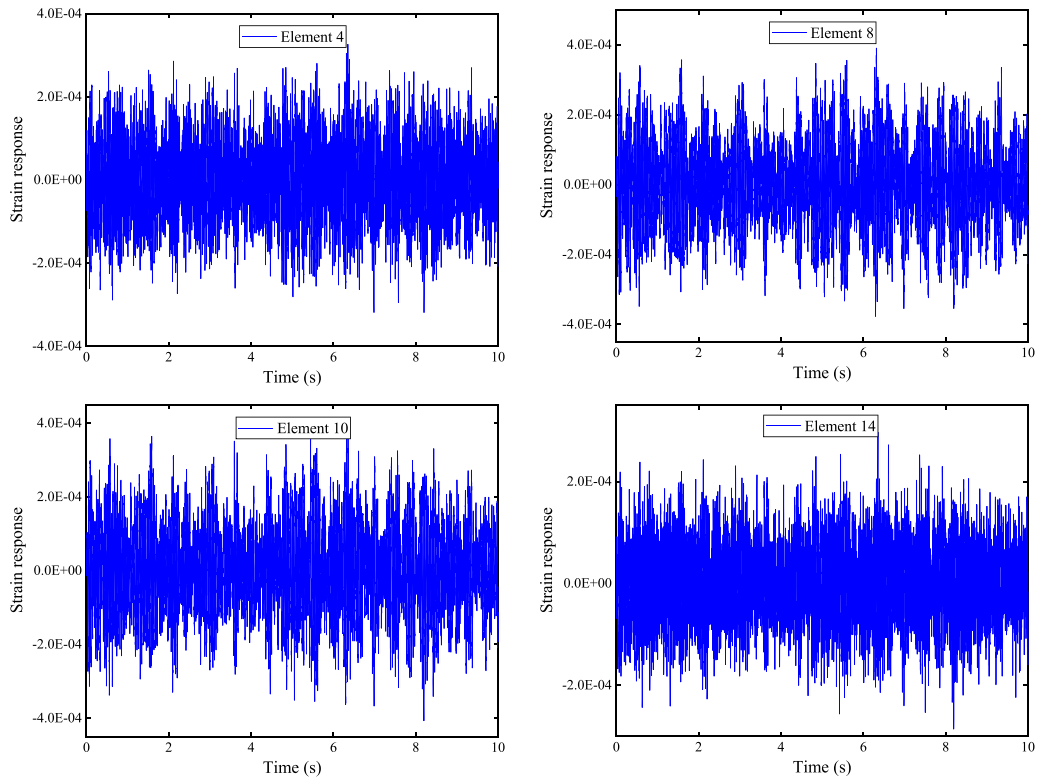


Figure 10. The strain response curves for damage case 2 (first 10 s).

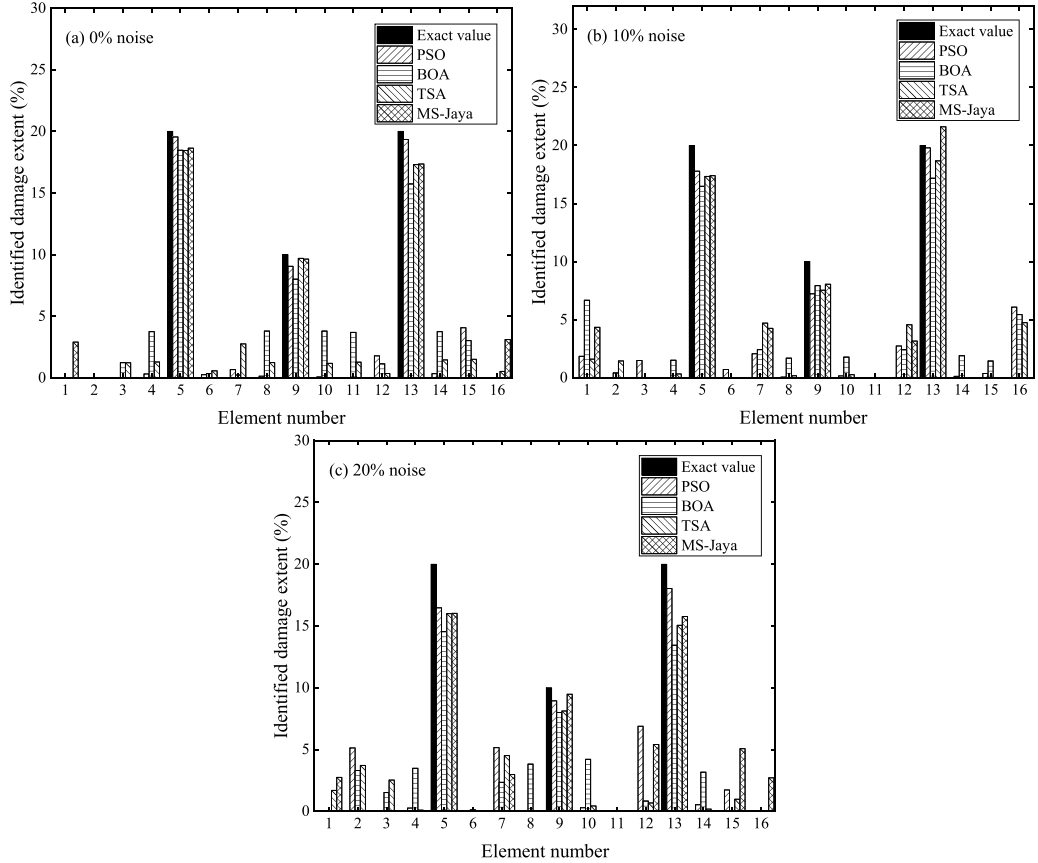


Figure 11. Identified results for damage case 2 under multiple excitations: (a) 0% noise; (b) 10% noise; (c) 20% noise.

Table 7. Mean and maximum errors for damage case 2 under multiple excitations (%).

Methods	0% noise		10% noise		20% noise	
	Mean error	Max error	Mean error	Max error	Mean error	Max error
PSO	0.81	4.07	1.58	6.08	1.97	6.88
BOA	2.17	4.25	2.40	6.67	2.55	6.55
TSA	1.22	2.76	1.71	4.74	1.80	4.95
MS-Jaya	0.79	3.11	1.31	4.34	1.94	5.41

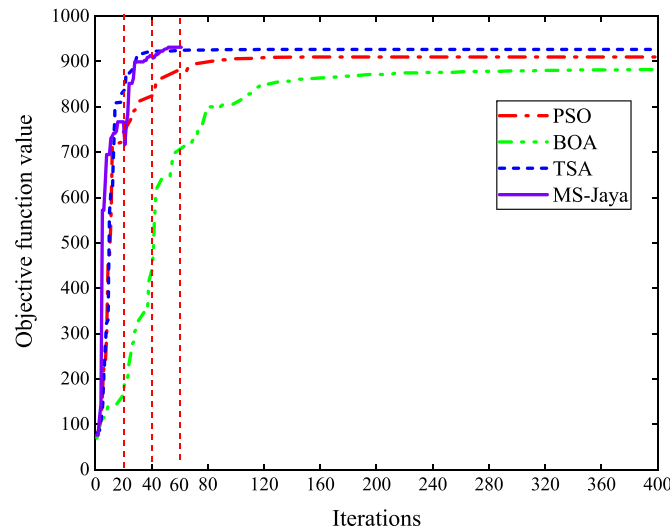


Figure 12. Convergence study for PSO, the BOA, the TSA, and MS-Jaya in damage case 2.

Table 8. Comparison of computational time for the proposed four methods under multiple excitations.

Methods	Objective value	Number of iterations	Computational time for single iteration (s)	Total time (s)
PSO	909.89	400	15.65	6260
BOA	882.23	400	15.75	6300
TSA	926.44	400	16.40	6557
MS-Jaya	931.65	60	16.41	985

results of damage locations and extent with maximum errors of less than 5.0% and 4.5% for the 10% noise case and 5.0% and 5.5% for the 20% noise case, which clearly prove the identification effectiveness and noise robustness of the proposed approaches.

Furthermore, the convergence performance and computational time for the proposed output-only damage identification methods are also investigated. As presented in figure 12, the TSA and MS-Jaya provide a relatively faster convergence rate, with around 60 iterations, than PSO and the BOA. As listed in table 8, the final objective function values of PSO, the BOA, the TSA, and MS-Jaya are 909.89, 882.23, 926.44, and 931.65, respectively. The total computation times of PSO, the BOA, and the TSA are 6260 s, 6300 s, and 6557 s, which is obviously longer than the 985 s consumed by the MS-Jaya algorithm. Therefore, the proposed MS-Jaya algorithm takes the least computational time but achieves the lowest objective function value among these four methods under ambient excitation.

In summary, from numerical studies of the simply supported beam structure, taking identification accuracy, computational efficiency, and noise robustness into consideration, the proposed output-only method based on swarm intelligence algorithms and correlation functions of strain responses can accurately detect, locate, and quantify damage with a limited number of sensors, multiple unknown ambient excitations, and seriously polluted measurements.

5. Validation with a benchmark structure

In recent years, considerable damage identification methods have been developed and validated by numerical and experimental research; however, these studies are basically based on different engineering structures and application conditions, rendering it quite difficult to evaluate the performance of diverse approaches. To deal with this issue, a bridge

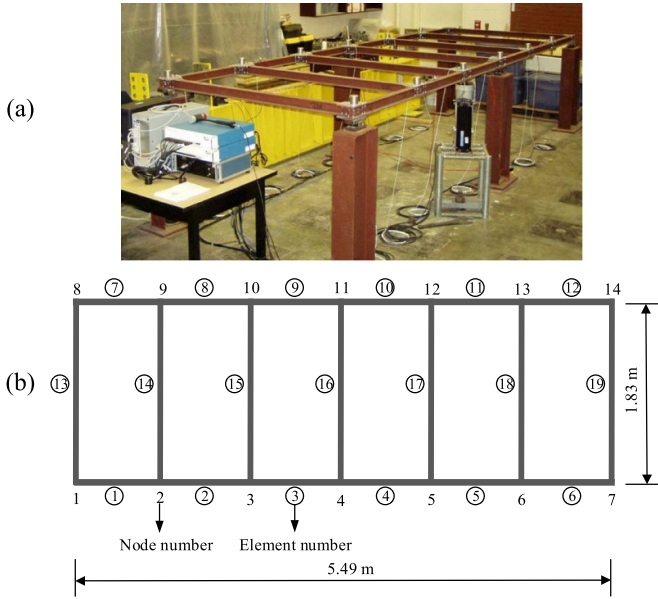


Figure 13. UCF grid benchmark structure: (a) experimental model; (b) finite element model.

benchmark model was established as a test bed to evaluate new techniques or methods for structural identification before real-life applications. In this section, a grid benchmark structure constructed at the University of Central Florida (UCF) is employed to validate the effectiveness of the proposed method.

5.1. Description of the grid benchmark structure

As shown in figure 13(a) [59], the UCF grid benchmark structure has a two-span continuous beam, and its total length and width are 5.49 m and 1.83 m. The girder and beams are $S3 \times 5.7$ standard sections, and piers are $W12 \times 26$ sections. The elastic modulus and mass density are $2.0 \times 10^{11} \text{ N m}^{-2}$ and 7850 kg m^{-3} , respectively.

The finite element model of the grid benchmark structure is shown in figure 13(b). There are 14 nodes and 19 elements. The boundary conditions of the support location, i.e. node numbers 1, 4, 7, 8, 11, and 14, are modeled as hinge connections that allow rotation in a certain direction and restrain the other degrees of freedom [60]. As shown in figure 14, the structure is excited by white noise excitations at nodes 2, 5, 10, and 13 in a vertical direction. Nine strain gauges are installed at the midpoint of elements 2, 4, 6, 7, 9, 11, 14, 16, and 18 to record dynamic responses for 600 s with a sampling frequency of 400 Hz. Measurement at the fourth element is treated as the reference point, resulting in nine sets of auto/cross-correlation function $R = [R_{4,2}, R_{4,4}, R_{4,6}, R_{4,7}, R_{4,9}, R_{4,11}, R_{4,14}, R_{4,16}, R_{4,18}]^T$. To test the capability of the proposed methods for detecting, localizing, and quantifying damage, two damage cases, i.e. single damage and multiple damages, are investigated. In the single damage case, 20% stiffness is reduced at the 15th element, namely, $\alpha_{15} = 0.2$. In the case of multiple damages, the stiffness of the

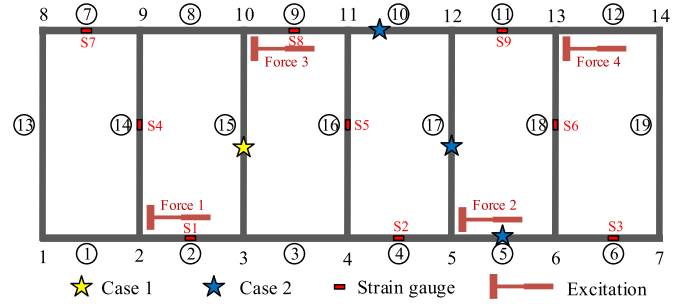


Figure 14. Setup of strain gauges and two damage cases.

fifth, 10th, and 17th elements are decreased by 20%, 10%, and 15%, namely, $\alpha_5 = 0.2, \alpha_{10} = 0.10$ and $\alpha_{17} = 0.15$.

5.2. Damage identification results

As displayed in figure 15 and table 9, the identified damage results of case 1 and case 2 clearly demonstrate that the proposed output-only identification strategy based on swarm intelligence algorithms, namely PSO, the BOA, the TSA, and MS-Jaya, with the correlation function of strain responses can detect damage location and extent, especially for the MS-Jaya algorithm. As table 9 shows, the maximum errors with MS-Jaya are 1.28% and 2.92% only in single and multiple damage cases, respectively, which indicates the superiority of the proposed MS-Jaya algorithm.

The MS-Jaya algorithm can achieve a superior value of the objective function with only 60 maximum iterations for two damage cases, i.e. single damage and multiple damages, as shown in table 10.

6. Discussion

6.1. Reference points

As illustrated in equation (11), the selection of reference points determines the auto/cross-correlation function of strain responses R , which may have an adverse effect on the performance of the proposed identification methods if an improper reference point is defined. Thus, the reference point plays an important role in damage identification. The simply supported beam structure in section 4.1 subjected to single white noise excitation is taken as a numerical example for a comparison study with different reference points. Four strain signals were measured at elements 4, 8, 10, and 14. By taking measurements at elements 4, 8, 10, and 14 as the reference points, four different sets of auto/cross correlation of strain responses are obtained, expressed as RP1, RP2, RP3, and RP4, respectively. The identified mean errors and maximum errors by PSO, the BOA, the TSA, and MS-Jaya with four different reference points are presented in table 11 and figure 16, respectively.

In table 11, it is observed that the identified mean errors of RP1 and RP4 are relatively larger than those acquired by RP2 and RP3, which implies that the performance of the correlation function-based method would be adversely affected. It

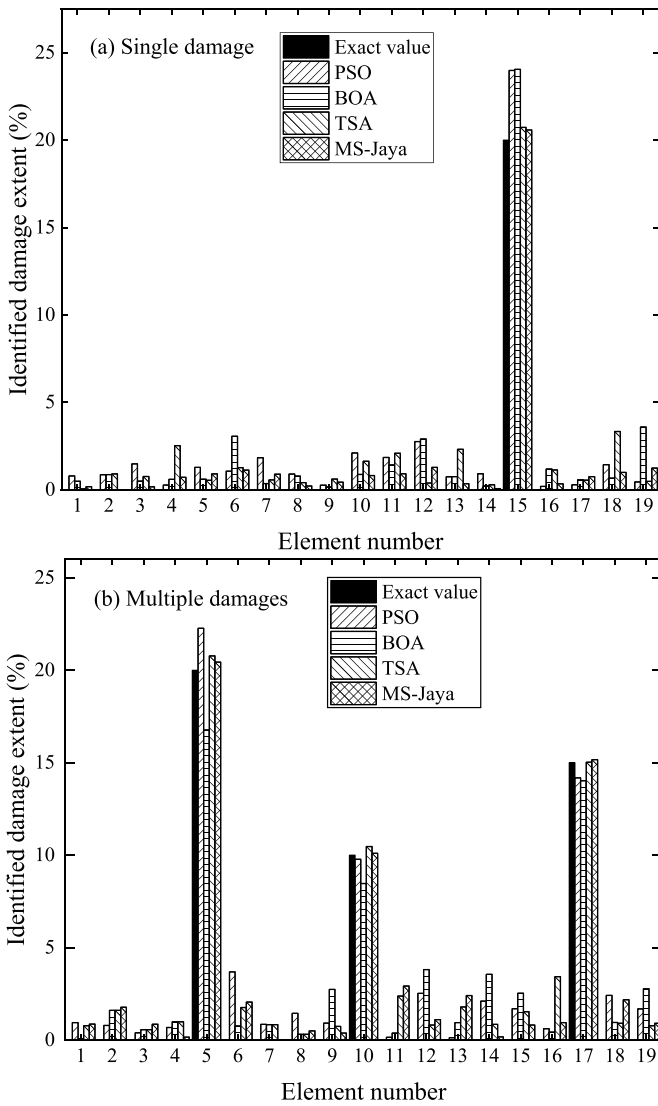


Figure 15. Identified damage extent of the benchmark structure: (a) single damage; (b) multiple damages.

Table 9. Identified error of the steel grid benchmark structure (%).

Methods	Single damage case		Multiple damages case	
	Mean error	Max error	Mean error	Max error
PSO	1.23	3.99	1.28	3.69
BOA	1.25	4.06	1.53	3.82
TSA	1.08	3.33	1.13	3.44
MS-Jaya	0.63	1.28	0.99	2.92

can be found from figure 16 that the maximum errors identified by PSO and the BOA with RP1 and RP4 are obviously larger than those with RP2 and RP3. Specifically, the BOA achieves apparently disappointing results with maximum errors of more than 9%, 12.5%, and 13.5% under 0%, 10%, and 20% noise for RP1. These results mean that PSO and the BOA have some difficulties in identifying the location and degree of structural

damage if an inappropriate reference point is selected. On the contrary, the proposed TSA and the MS-Jaya algorithm can provide satisfactory identification results with all reference points. The worst results of less than 8.0% and 7.5% maximum errors are obtained by the TSA and MS-Jaya with RP1 under 20% noise, which indicates that the selection of different reference points has a modest effect on the computational results owing to their powerful global exploration and local exploitation capacity.

Therefore, it can be concluded that the selection of reference points would not significantly affect the identification results for the stronger algorithms, i.e. the TSA and MS-Jaya, but would evidently affect the performance of the weaker algorithms, i.e. PSO and the BOA.

6.2. Number of sensors

Generally, a robust method is desired to accurately identify structural damage with as few sensors as possible. Thus, in this section, the robustness of the proposed output-only method to the number of sensors is discussed with the numerical example of the simply supported beam in section 4.1. As listed in table 12, four different numbers of sensors, i.e. 2, 3, 4, and 5, are employed and compared. Obviously, as the number of sensors increases, more data points of the correlation function of strain responses R are involved. The final identified results by the TSA for four different sensor settings are shown in figure 17 and table 13.

It is clearly observed from figure 17 that the identified errors of damage variables decrease accordingly with the increasing number of sensors. However, there will be a small variation in identified errors but an apparent increase in computational time, as presented in table 13, if more than three sensors are utilized, which indicates that using excessive sensors may not significantly improve identification accuracy but definitely consumes considerable computational time. Therefore, within the range of acceptable error, the number of sensors should be selected reasonably in order to save computational resources.

6.3. Detectable range of strain sensor

Although the applicability and effectiveness of the strain response-based method have been validated in numerical and experimental studies, the detectable range of the strain sensor may still pose some difficulties in real applications. In fact, damage locations cannot always appear in the detection range of a strain sensor [31]. Thus, the effect of the detectable range of the strain sensor on the identification results needs to be further investigated. Five different arrangements of strain gauges on the simply supported beam structure are considered. In case 1(a), four strain gauges are installed at the midpoints of elements 4, 8, 10, and 14 along the upper surface of the beam, as shown in figure 6; in case 1(b), four strain gauges are installed at the midpoints of elements 4, 7, 11, 14; in case 1(c), four strain gauges are installed at the midpoints of elements 4, 6, 12, and 14; in case 1(d), four strain gauges are installed at the

Table 10. Objective value and number of iterations for PSO, the BOA, the TSA, and MS-Jaya.

Methods	Single damage case		Multiple damages case	
	Objective value	Number of iterations	Objective value	Number of iterations
PSO	854.16	400	857.72	400
BOA	848.43	400	821.99	400
TSA	901.42	400	894.54	400
MS-Jaya	955.70	60	934.49	60

Table 11. Identified mean errors based on four methods with RP1, RP2, RP3, and RP4.

Noise level	Reference points			
	RP1	RP2	RP3	RP4
Noise free	1.36	1.06	0.77	1.60
10% noise	1.64	1.25	0.97	1.48
20% noise	1.98	1.74	1.41	2.04

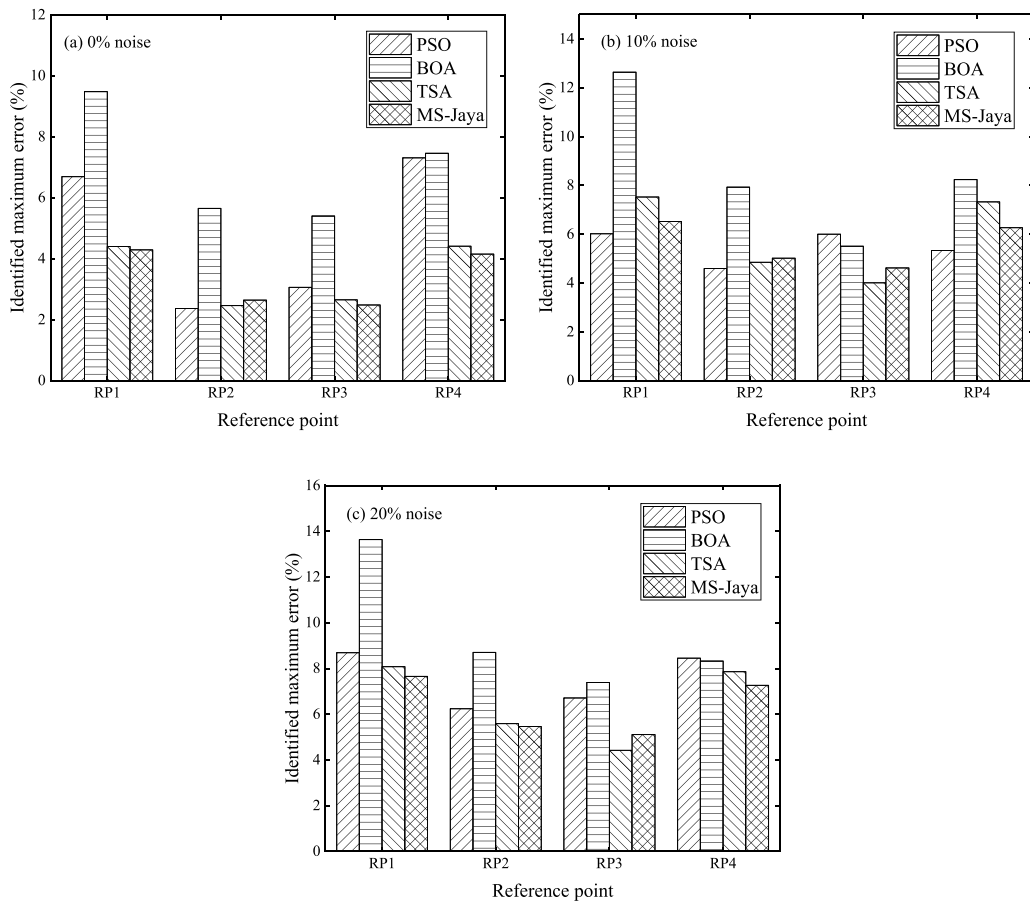


Figure 16. Identified maximum errors with different reference points: (a) 0% noise; (b) 10% noise; (c) 20% noise.

midpoints of elements 3, 5, 13, and 15; in case 1(e), four strain gauges are installed at the midpoints of elements 2, 3, 14, and 15. We assume there is a 15% reduction in Young’s modulus at element 9, and the strain response from the second sensor S2 is selected as the reference point. The damage detection results with the TSA are presented in figure 18.

In figure 18, it is clearly observed that the damage location and magnitude are accurately detected for case 1(a), case 1(b), and case 1(c) with the maximum errors of 1.79%, 2.86%, and 2.71%, respectively. In case 1(d), the identified results of healthy elements were inferior to those of the damaged element since the maximum identification error

Table 12. The setting of measurements and reference points with different sensors.

Number of sensors	Measurement	Reference point	Correlation function of strain responses R
2	4, 10	2	$R = [R_{10,4}, R_{10,10}]$
3	4, 10, 14	2	$R = [R_{10,4}, R_{10,10}, R_{10,14}]$
4	4, 8, 10, 14	3	$R = [R_{10,4}, R_{10,8}, R_{10,10}, R_{10,14}]$
5	2, 4, 8, 10, 14	4	$R = [R_{10,2}, R_{10,4}, R_{10,8}, R_{10,10}, R_{10,14}]$

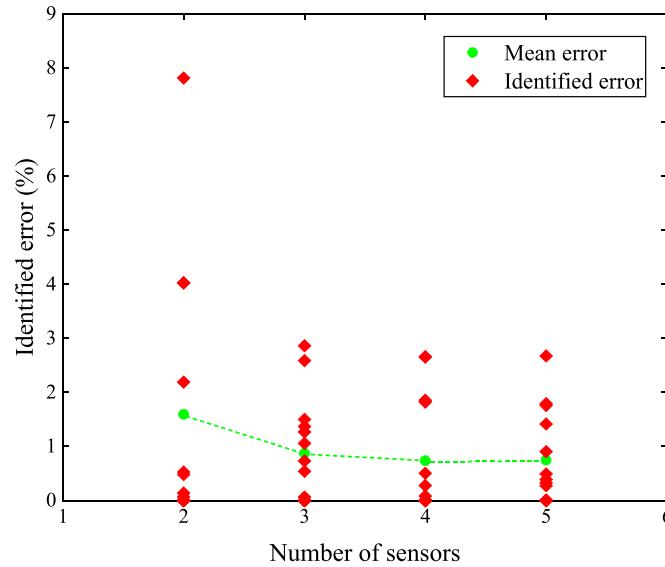


Figure 17. Identified errors by the TSA for four sensor settings (noise free).

Table 13. Identification results and computational time with different numbers of sensors (%).

Number of sensors	0% noise		10% noise		20% noise		Computational time (s)
	Mean	Maximum	Mean	Maximum	Mean	Maximum	
2	1.59	7.82	2.19	7.47	2.54	9.94	1818
3	0.87	2.86	1.01	3.85	1.62	6.44	1946
4	0.74	2.65	0.85	4.00	1.20	4.42	2132
5	0.75	2.67	0.84	5.02	1.30	5.59	2269

of 4.71% appears at intact element 8. For the worst case 1(e), the identified damage extent obviously deviates from the actual value with a maximum error of around 7.2% owing to the adverse effect of a lack of nearby strain sensors. These results demonstrate that the proposed correlation function of strain responses has favorable robustness to the

arrangement of sensors, while false identification may be acquired when the location of damage is too far from the strain sensor. Considering the limitations of the detectable range of strain sensors, it is suggested that the installment of strain gauges should be optimized to identify structural damage.

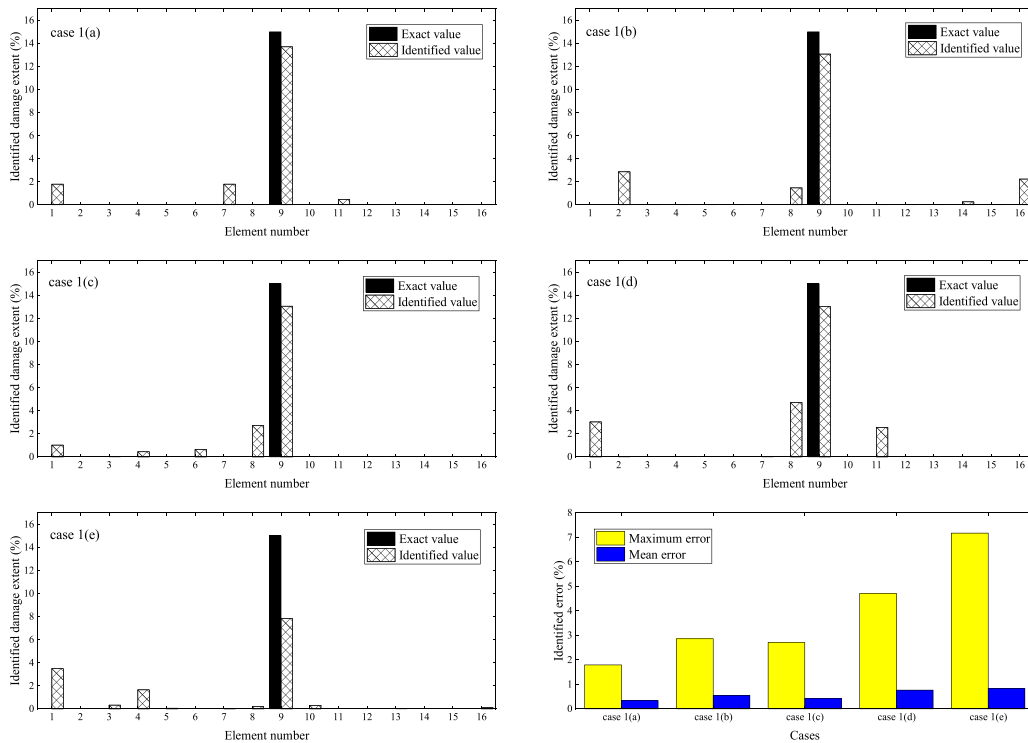


Figure 18. The identified damage results for case 1(a), case 1(b), case 1(c), case 1(d), and case 1(e).

7. Conclusions

In this paper, an output-only structural damage identification approach based on swarm intelligence algorithms and correlation functions of strain responses is proposed when a structure is subjected to single or multiple unknown white noise excitations. Four different swarm intelligence algorithms, i.e. PSO, the BOA, the TSA, and MS-Jaya are employed and compared. A penalty function is integrated into the objective function to alleviate false alarm identification. Numerical studies on a simply supported beam structure and a steel grid benchmark structure are implemented to demonstrate the accuracy, efficiency, and robustness of the proposed approach. Based on the reliable results of studies as well as discussions on reference points, number of sensors, and detectable range of strain sensors, some interesting conclusions can be summarized, as follows:

(1) Taking the identification accuracy, computational efficiency, and noise robustness into consideration, compared with PSO, the BOA, and the TSA, the proposed MS-Jaya algorithm can achieve better performance owing to integrating an MS mechanism by successively eliminating the intact elements during the iteration process.

(2) The proposed output-only method with four different swarm intelligence algorithms and correlation functions of strain responses can accurately detect, locate, and quantify

structural damage using a limited number of sensors and seriously polluted measurements, implying the favorable compatibility of the proposed approach with various optimization algorithms.

(3) The selection of reference points would not significantly change the performance for algorithms with stronger search capacity, such as the TSA and MS-Jaya, but would evidently affect the effectiveness of algorithms with weaker search capacity, such as PSO and the BOA.

(4) Identifying structural damage with excessive sensors has a negligible effect on identification accuracy but inevitably consumes considerable computational time. Within the allowable range of identified error, the number of sensors should be reasonably selected.

(5) The strain measurements are more sensitive to local damage, while the detectable range of strain sensors limits their capacity for damage identification. It is necessary to optimize the placement of strain gauges to improve the ability of damage identification.

The limitation is that relatively simple linear structural systems are identified using the proposed approach. The outlook for future work is that modeling errors and temperature variation should be considered in damage identification in more complex and large-scale civil structures in future studies.

Data availability statement


All data that support the findings of this study are included within the article (and any supplementary files).

Acknowledgments

This work was supported by the National Key R&D Program of China (2021YFE0112200), the Japan Society for Promotion of Science (Kakenhi No. 18K04438), the Tohoku Institute of Technology Research Grant, and the Postgraduate Research & Practice Innovation Program of Jiangsu Province (KYCX23_0273). This financial support is sincerely appreciated. The authors would also like to thank the anonymous reviewers for their detailed and fruitful remarks.

ORCID iDs

Kun Feng  <https://orcid.org/0000-0003-1110-3681>

Chunfeng Wan  <https://orcid.org/0000-0002-4236-6428>

Liyu Xie  <https://orcid.org/0000-0001-5777-0645>

References

- [1] Fan W and Qiao P 2011 Vibration-based damage identification methods: a review and comparative study *Struct. Health Monit.* **10** 83–111
- [2] Chang P C, Flatau A and Liu S C 2003 Health monitoring of civil infrastructure *Struct. Health Monit.* **2** 257–67
- [3] Yan Y J, Cheng L, Wu Z Y and Yam L H 2007 Development in vibration-based structural damage detection technique *Mech. Syst. Signal Process.* **21** 2198–211
- [4] Sha G G, Radziński M, Cao M and Ostachowicz W 2019 A novel method for single and multiple damage detection in beams using relative natural frequency changes *Mech. Syst. Signal Process.* **132** 335–52
- [5] Görl E and Link M 2003 Damage identification using changes of eigenfrequencies and mode shapes *Mech. Syst. Signal Process.* **17** 103–10
- [6] Nguyen K-D, Chan T H T and Thambiratnam D P 2016 Structural damage identification based on change in geometric modal strain energy–eigenvalue ratio *Smart Mater. Struct.* **25** 075032
- [7] Roy K 2017 Structural damage identification using mode shape slope and curvature *J. Eng. Mech.* **143** 04017110
- [8] Zhang J, Li P J and Wu Z S 2013 A new flexibility-based damage index for structural damage detection *Smart Mater. Struct.* **22** 025037
- [9] Du D-C, Vinh H-H, Trung V-D, Hong Quyen N-T and Trung N-T 2018 Efficiency of Jaya algorithm for solving the optimization-based structural damage identification problem based on a hybrid objective function *Eng. Optim.* **50** 1233–51
- [10] Farrar C R and Doebling S W 1997 Lessons learned from applications of vibration-based damage identification methods to a large bridge structure *Proc. Int. Workshop on Structural Health Monitoring* (Stanford University) pp 351–70
- [11] Perry M J and Koh C G 2008 Output-only structural identification in time domain: numerical and experimental studies *Earthquake Eng. Struct. Dyn.* **37** 517–33
- [12] Yang J N, Huang H W and Lin S L 2006 Sequential non-linear least-square estimation for damage identification of structures *Int. J. Non-Linear Mech.* **41** 124–40
- [13] Zhang X, Wan S T, He Y L, Wang X L and Dou L J 2021 Teager energy spectral kurtosis of wavelet packet transform and its application in locating the sound source of fault bearing of belt conveyor *Measurement* **173** 108367
- [14] Xue S T, Tang H S and Xie Q 2009 Structural damage detection using auxiliary particle filtering method *Struct. Health Monit.* **8** 101–12
- [15] Lu Z-R and Wang L 2017 An enhanced response sensitivity approach for structural damage identification: convergence and performance *Int. J. Numer. Methods Eng.* **111** 1231–51
- [16] Xu B and He J 2015 Substructural parameters and dynamic loading identification with limited observations *Smart Struct. Syst.* **15** 169–89
- [17] Zhu H-P, Mao L and Weng S 2014 A sensitivity-based structural damage identification method with unknown input excitation using transmissibility concept *J. Sound Vib.* **333** 7135–50
- [18] Jayalakshmi V and Rao A 2017 Simultaneous identification of damage and input dynamic force on the structure for structural health monitoring *Struct. Multidiscipl. Optim.* **55** 2211–38
- [19] Xu B, He J, Rovekamp R and Dyke S J 2012 Structural parameters and dynamic loading identification from incomplete measurements: approach and validation *Mech. Syst. Signal Process.* **28** 244–57
- [20] Ni P H, Yin Z Y, Han Q and Du X L 2023 Output-only structural identification with random decrement technique *Structures* **51** 55–66
- [21] Wang X J, Chen F, Zhou H Y, Ni P, Wang L and Zhang J 2022 Structural damage detection based on cross-correlation function with data fusion of various dynamic measurements *J. Sound Vib.* **541** 117373
- [22] Ni P H, Wang X J and Zhou H Y 2021 Output-only structural damage detection under multiple unknown white noise excitations *Struct. Eng. Mech.* **79** 327–36
- [23] Yang Z C, Yu Z F and Sun H 2007 On the cross correlation function amplitude vector and its application to structural damage detection *Mech. Syst. Signal Process.* **21** 2918–32
- [24] Li X Y and Law S S 2010 Matrix of the covariance of covariance of acceleration responses for damage detection from ambient vibration measurements *Mech. Syst. Signal Process.* **24** 945–56
- [25] Ni P H, Xia Y, Law S-S and Zhu S Y 2014 Structural damage detection using auto/cross-correlation functions under multiple unknown excitations *Int. J. Struct. Stab. Dyn.* **14** 1440006
- [26] Zhang G C, Wan C F, Xiong X B, Xie L Y, Noori M and Xue S T 2022 Output-only structural damage identification using hybrid Jaya and differential evolution algorithm with reference-free correlation functions *Measurement* **199** 111591
- [27] Yam L Y, Leung T P, Li D B and Xue K Z 1996 Theoretical and experimental study of modal strain analysis *J. Sound Vib.* **192** 251–60
- [28] Liu L J, Zhang X and Lei Y 2023 Data-driven identification of structural damage under unknown seismic excitations using the energy integrals of strain signals transformed from transmissibility functions *J. Sound Vib.* **546** 117490
- [29] Xu Z-D and Wu K-Y 2012 Damage detection for space truss structures based on strain mode under ambient excitation *J. Eng. Mech.* **138** 1215–23
- [30] Li X H, Kurata M and Nakashima M 2015 Evaluating damage extent of fractured beams in steel moment-resisting frames using dynamic strain responses *Earthquake Eng. Struct. Dyn.* **44** 563–81

- [31] Cui H Y, Xu X, Peng W Q, Zhou Z H and Hong M 2018 A damage detection method based on strain modes for structures under ambient excitation *Measurement* **125** 438–46
- [32] Shadan F, Khoshnoudian F and Esfandiari A 2018 Structural damage identification based on strain frequency response functions *Int. J. Struct. Stab. Dyn.* **18** 1850159
- [33] Zhang S X, Wang Z Y, Jian Z K, Liu G Y and Liu X J 2020 A two-step method for beam bridge damage identification based on strain response reconstruction and statistical theory *Meas. Sci. Technol.* **31** 075008
- [34] Li M, Ren W-X, Huang T-L and Wang N-B 2020 Experimental investigations on the cross-correlation function amplitude vector of the dynamic strain under varying environmental temperature for structural damage detection *J. Low Freq. Noise Vib. Act. Control* **39** 631–49
- [35] Lyu Y T, Yang J W, Ge M and Xu L 2023 Wavelet packet energy-based damage detection using guided ultrasonic waves and support vector machine *Meas. Sci. Technol.* **34** 075107
- [36] Zhang C L, Dou D Y, Sun F J and Huang Z X 2022 Detecting coal content in gangue via machine vision and genetic algorithm-backpropagation neural network *Measurement* **201** 111739
- [37] Kaveh A and Eslamlou A D 2019 An efficient two-stage method for optimal sensor placement using graph-theoretical partitioning and evolutionary algorithms *Struct. Control Health Monit.* **26** e2325
- [38] Feng K, González A and Casero M 2021 A kNN algorithm for locating and quantifying stiffness loss in a bridge from the forced vibration due to a truck crossing at low speed *Mech. Syst. Signal Process.* **154** 107599
- [39] Xia Z Y, Li A Q, Li J H, Shi H Y, Duan M J and Zhou G P 2020 Model updating of an existing bridge with high-dimensional variables using modified particle swarm optimization and ambient excitation data *Measurement* **159** 107754
- [40] Seyedpoor S M and Nopour M H 2020 A two-step method for damage identification in moment frame connections using support vector machine and differential evolution algorithm *Appl. Soft Comput.* **88** 106008
- [41] Kaveh A, Vaez S R H, Hosseini P and Fallah N 2016 Detection of damage in truss structures using simplified dolphin echolocation algorithm based on modal data *Smart Struct. Syst.* **18** 983–1004
- [42] Zhou H Y, Zhang G C, Wang X J, Ni P H and Zhang J 2021 Structural identification using improved butterfly optimization algorithm with adaptive sampling test and search space reduction method *Structures* **33** 2121–39
- [43] Hosseinzadeh A Z, Bagheri A, Amiri G G and Koo K Y 2014 A flexibility-based method via the iterated improved reduction system and the cuckoo optimization algorithm for damage quantification with limited sensors *Smart Mater. Struct.* **23** 045019
- [44] Ding Z H, Li J, Hao H and Lu Z-R 2019 Structural damage identification with uncertain modelling error and measurement noise by clustering based tree seeds algorithm *Eng. Struct.* **185** 301–14
- [45] Das S and Saha P 2021 Performance of swarm intelligence based chaotic meta-heuristic algorithms in civil structural health monitoring *Measurement* **169** 108533
- [46] Zhou H Y, Zhang G C, Wang X J, Ni P H and Zhang J 2020 A hybrid identification method on butterfly optimization and differential evolution algorithm *Smart Struct. Syst.* **26** 345–60
- [47] Khatir S, Wahab M A, Boutchicha D and Khatir T 2019 Structural health monitoring using modal strain energy damage indicator coupled with teaching-learning-based optimization algorithm and isogeometric analysis *J. Sound Vib.* **448** 230–46
- [48] Huang M S, Cheng X H and Lei Y Z 2021 Structural damage identification based on substructure method and improved whale optimization algorithm *J. Civ. Struct. Health Monit.* **11** 351–80
- [49] Kaveh A, Hosseini S M and Zaerreza A 2021 Improved shuffled Jaya algorithm for sizing optimization of skeletal structures with discrete variables *Structures* **29** 107–128
- [50] Zhang G C, Wan C F, Xue S T and Xie L Y 2023 A global-local hybrid strategy with adaptive space reduction search method for structural health monitoring *Appl. Math. Model.* **121** 231–51
- [51] Ding Z H, Li J and Hao H 2019 Structural damage identification using improved Jaya algorithm based on sparse regularization and Bayesian inference *Mech. Syst. Signal Process.* **132** 211–31
- [52] Ding Z H, Yu Y, Tan D and Yuen K-V 2023 Adaptive vision feature extractions and reinforced learning-assisted evolution for structural condition assessment *Struct. Multidiscipl. Optim.* **66** 209
- [53] Gerist S and Maheri M R 2016 Multi-stage approach for structural damage detection problem using basis pursuit and particle swarm optimization *J. Sound Vib.* **384** 210–26
- [54] Norrie D H and de Vries G 1978 *An Introduction to Finite Element Analysis* (Academic)
- [55] Kennedy J and Eberhart R C 1995 Particle swarm optimization *IEEE Int. Conf. on Neural Networks (Perth, Australia)* pp 1942–8
- [56] Arora S and Singh S 2019 Butterfly optimization algorithm: a novel approach for global optimization *Soft Comput.* **23** 715–34
- [57] Kiran M S 2015 TSA: tree-seed algorithm for continuous optimization *Expert Syst. Appl.* **42** 6686–98
- [58] Shi Y H and Eberhart R C, Empirical study of particle swarm optimization *Proc. IEEE Congress on Evolutionary Computation (Washington, DC, USA, 6–9 July 1999)* pp 1945–50
- [59] Catbas F N, Gul M and Burkett J L 2008 Conceptual damage-sensitive features for structural health monitoring: laboratory and field demonstrations *Mech. Syst. Signal Process.* **22** 1650–69
- [60] Abdeljaber O and Avcı O 2016 Nonparametric structural damage detection algorithm for ambient vibration response: utilizing artificial neural networks and self-organizing maps *J. Archit. Eng.* **22** 04016004